

# Hole-assisted lightguide fibers with small negative dispersion and low dispersion slope

Dora Juan Juan Hu,<sup>1,\*</sup> Ping Shum,<sup>1</sup> Guobin Ren,<sup>1</sup> and Chao Lu<sup>2</sup>

<sup>1</sup>School of Electrical and Electronic Engineering, Nanyang Technological University, Singapore

<sup>2</sup>Department of Electronic and Information Engineering, Hong Kong Polytechnic University, Hong Kong

\*Corresponding author: hujuanjuan@pmail.ntu.edu.sg

Received 13 June 2008; revised 9 August 2008; accepted 19 August 2008;  
posted 21 August 2008 (Doc. ID 97393); published 19 September 2008

A nonzero dispersion shifted fiber design based on hole-assisted lightguide fiber is presented. The proposed fiber has low dispersion slope around  $-0.01 \text{ ps/nm}^2\text{-km}$  and small negative dispersion values over the wavelength range from 1530 to 1620 nm. It can be used as a transmission medium for a long-haul dense wavelength-division-multiplexed system. © 2008 Optical Society of America

OCIS codes: 060.0060, 060.5295.

## 1. Introduction

Exploitation of air holes in optical fiber design has been an active research topic since the first demonstration of the photonic crystal fiber (PCF) by Knight *et al.* [1]. Air-silica PCFs possess a microstructured array of air holes in the cladding that run uniformly along the fiber axis. The holey structure allows more flexibility in the fiber design for achieving many uncommon optical properties such as broadband single mode transmission, group velocity dispersion tailoring, enhanced nonlinearity, and guidance by a hollow core through the photonic bandgap effect [2]. Introduced by Hasegawa *et al.*, hole-assisted lightguide fiber (HALF) is an optical fiber with a high index core encircled by a few assisted air holes in a low index cladding [3]. Like conventional optical fibers, the guiding mechanism for HALF is total internal reflection. The existence of the air holes does not aim to vary the guiding mechanism but to modify the optical properties such as dispersion characteristics. Compared to the other microstructured fibers such as PCFs, HALFs are easier to fabricate and handle due to less complexity in the cladding. Owing to the contributions of the large index contrast between air and silica, HALFs are proposed to achieve many

parameters by utilizing the assisting air holes. The scattering loss is greatly reduced due to less air-silica interface in HALFs. In addition, excellent bending loss characteristics have been reported for such fibers [4]. Previous studies have demonstrated that HALF can exhibit large anomalous dispersion unattainable by conventional optical fibers. The loss observed in the experiment is as low as comparable to conventional optical fibers [3]. HALFs are also proposed to obtain a large negative dispersion coefficient with low scattering loss [5]. With proper structure design, modifications of dispersion properties such as small dispersion values with flat dispersion slope could be obtained [6]. In this paper, we propose a negative nonzero dispersion shifted fiber (NZ-DSF) design based on HALF. The small negative dispersion values with low dispersion slope around  $-0.01 \text{ ps/nm}^2\text{-km}$  are achieved over the wavelength range from 1530 to 1620 nm, which makes the proposed HALF a suitable candidate of transmission medium for long-haul dense wavelength-division-multiplexed (DWDM) systems. The advantage of the proposed design is that in long-haul transmission systems, the accumulated negative dispersion values of the transmission fiber can be easily compensated by standard single mode fibers (SSMF). Compared to other NZ-DSF designs with positive dispersion values such as the one in [6], the proposed design eliminates the possible use of dispersion compensating

fibers, which have the disadvantages of large attenuation and strong nonlinearity effects.

## 2. Fiber Design

Triclad structure has been investigated for dispersion tailoring characteristics with potential applications of dispersion compensation fiber or transmission fiber with flattened small dispersion values [7,8]. As illustrated in Fig. 1, the refractive index profile of the proposed fiber design has the following parameters: central depressed core diameter  $2a_0$ , core diameter  $2a$ , depressed cladding diameter  $2b$ , which is surrounded by a raised index region  $2c$ , and refractive index differences  $\Delta n_0$ ,  $\Delta n_1$ ,  $\Delta n_2$ , and  $\Delta n_3$  compared to the background material. The central index depression  $\Delta n_0$  in the core region helps to expand the effective mode area of the fiber, which is desirable to reduce fiber nonlinearity in long-haul transmission. The depressed cladding layer would reduce the waveguide dispersion. The outer cladding contributes to a larger effective core area and improvements of bending loss. With appropriate selections of the refractive index and the width of the depressed cladding layer

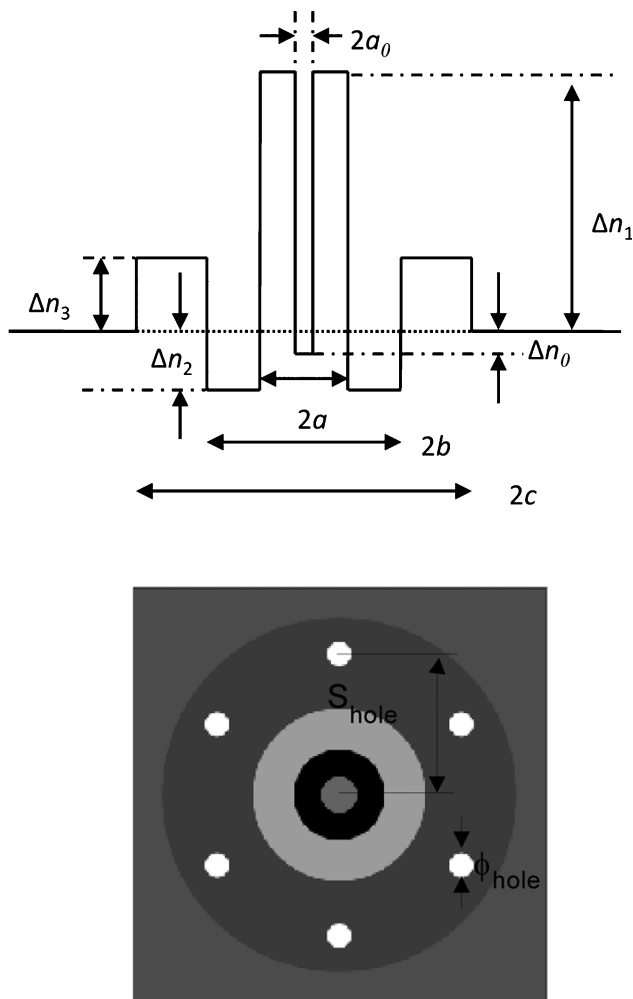


Fig. 1. Refractive index profile of the proposed NZ-DSF design based on HALF. The gray level corresponds to the refractive index level.

and the outer cladding layer, dispersion flattening could be achieved. Based on the tri-clad structure, the proposed NZ-DSF design has a few air holes that are placed in the outer cladding layer. The hole diameter and hole to core separation are denoted as  $\Phi_{\text{hole}}$  and  $S_{\text{hole}}$ , respectively. The gray level corresponds to the refractive index level. The parameters in the proposed design are as follows:  $2a_0 = 3.0 \mu\text{m}$ ,  $2a = 7.5 \mu\text{m}$ ,  $2b = 14.25 \mu\text{m}$ ,  $2c = 29.25 \mu\text{m}$ ,  $\Delta n_0 = -0.1\%$ ,  $\Delta n_1 = 0.44\%$ ,  $\Delta n_2 = -0.32\%$  and  $\Delta n_3 = 0.1\%$ ,  $\Phi_{\text{hole}} = 1.0 \mu\text{m}$ , and  $S_{\text{hole}} = 11.625 \mu\text{m}$ .

## 3. Results and Analysis

Figure 2 presents the mode index  $n_{\text{eff}}$  curve as a function of wavelength. The solid curve represents the  $n_{\text{eff}}$  curve of the proposed NZ-DSF design based on HALF, and the dotted curve is the  $n_{\text{eff}}$  curve of the tri-clad structure without the incorporation of air holes. The calculations are done using the scalar beam propagation method (BPM) developed by RSOFT Design Group, Inc. The two curves are found to be significantly different at longer wavelength. Specifically, the dotted curve becomes more flattened as one approaches the background refractive index 1.45, i.e., the rate of change is getting slower. This effect results from the incorporation of the assisting air holes in the outer cladding layer. As qualitatively explained in [8], the mode coupling from the core to the outer cladding layer becomes more significant in longer wavelengths. Due to the raised index of the outer cladding layer, the fundamental mode index therefore decreases at a slower speed. The influence of the outer cladding layer is alleviated because there is certain portion of the lightwave residing in the air holes. However, it is found that the air holes are actually expelling the lightwave, i.e., a smaller portion is coupled into the outer cladding layer, therefore offsetting the influence of the higher-index outer cladding, i.e., the mode index decreases at a faster speed.

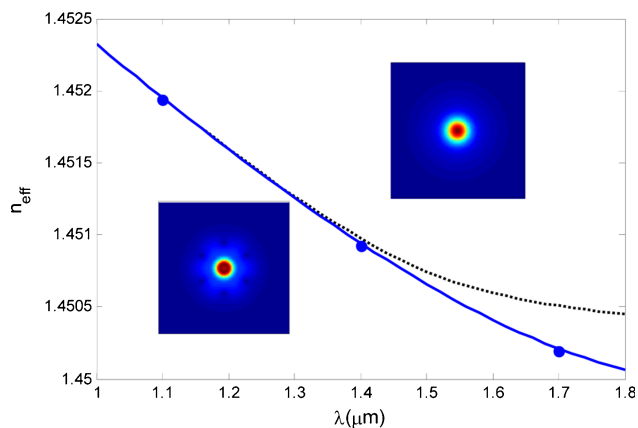


Fig. 2. (Color online) Effective index curves of the proposed HALF (solid line) and the tri-clad structure without air holes (dotted line). The shaded dots are the effective index obtained by full vectorial BPM at  $\lambda = 1.1$ ,  $1.4$ , and  $1.7 \mu\text{m}$ , respectively. The insets show the mode profiles at  $\lambda = 1.55 \mu\text{m}$  for the HALF (lower inset) and the tri-clad structure without air holes (upper inset).

This phenomenon can be seen from the Fig. 2 inset plots of the mode profile at 1550 nm for both structures. The effective mode area is around  $86.2 \mu\text{m}^2$  for the proposed HALF. If the central index depression  $\Delta n_0$  is zero, the effective mode area is  $46.9 \mu\text{m}^2$ , which would result in greater nonlinearity than the proposed design. The cutoff wavelength is found to be around 560 nm. At longer wavelengths, the higher-order modes become very leaky and single mode operation in the *C*- and *L*-bands is guaranteed. Additionally, the shaded dots are obtained by full vectorial BPM, and they are found in good agreement with the curve obtained by the scalar BPM in the analysis.

The dispersion characteristics of this fiber are illustrated in Fig. 3. Material dispersion is included in the calculation. The dispersion values are calculated from Fig. 2  $n_{\text{eff}}$  curves. The solid line is the dispersion curve of the proposed HALF design. It can be seen that negative flat dispersion is obtained in the wavelength range from 1530 to 1620 nm. Specifically, the dispersion slope is around  $-0.01 \text{ ps/nm}^2\text{-km}$ . The negative dispersion values are within the range of  $(-1.2, -0.2) \text{ ps/nm-km}$ . The zero dispersion wavelength is around  $1.7 \mu\text{m}$  as shown in the inset magnified plot. For the use of the proposed HALF in the long-haul DWDM transmission system, the accumulated negative dispersion values can be conveniently compensated by a standard single mode fiber. The dispersion slope compensation can be eliminated due to the low dispersion slope of the proposed structure. The dash-dotted curve represents the dispersion curve for the tri-clad structure without air holes. It can be seen that beyond the wavelength of  $1.3 \mu\text{m}$ , the dispersion value varies drastically. It can be understood that the dispersion value is linked to the second-order derivatives of the mode index  $n_{\text{eff}}$ . As shown in Fig. 2, the variation of the mode in-

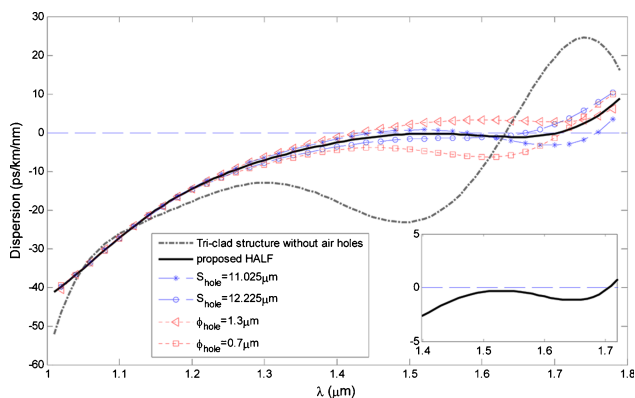


Fig. 3. (Color online) Dispersion curves. Solid curve, the proposed HALF design (inset shows the magnified view). The flat low dispersion is obtained in the *C*- and *L*-bands. The negative dispersion values are within  $(-1.2, -0.2) \text{ ps/nm-km}$ , and the dispersion slope is around  $-0.01 \text{ ps/nm}^2\text{-km}$ . Dashed-dotted curve, tri-clad structure without the air holes; star/circle solid curves, the proposed HALF structure except  $S_{\text{hole}} = 11.025 \mu\text{m}/12.225 \mu\text{m}$ ; triangle/square dashed lines, the proposed HALF structure except  $\Phi_{\text{hole}} = 1.3 \mu\text{m}/0.7 \mu\text{m}$ .

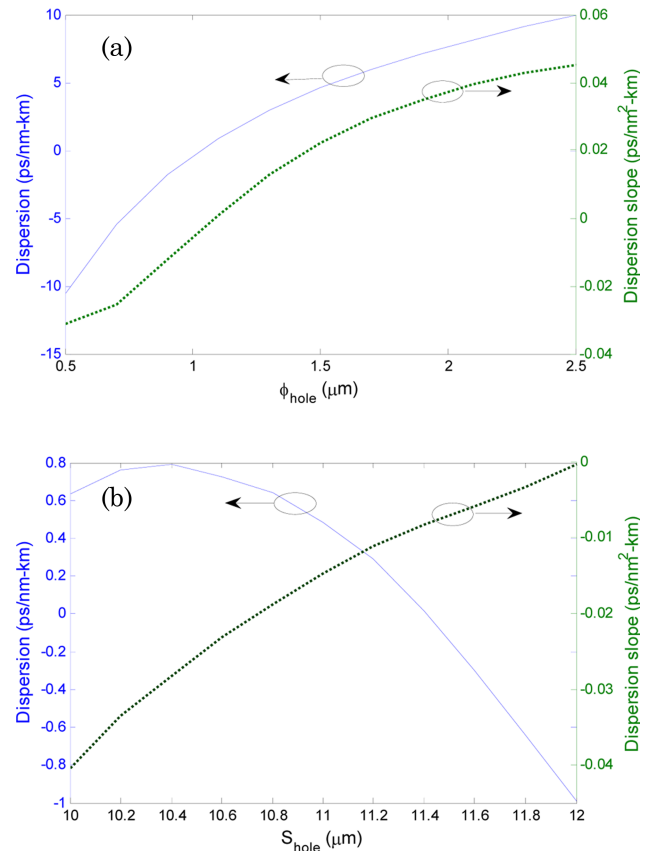


Fig. 4. (Color online) Dispersion values (solid lines) and dispersion slope (dotted lines) at  $\lambda = 1.55 \mu\text{m}$  as functions of (a) air hole diameter  $\Phi_{\text{hole}}$ , (b) air hole position  $S_{\text{hole}}$ .

dex  $n_{\text{eff}}$  curve for the tri-clad structure “slows down” beyond  $1.3 \mu\text{m}$ , which results in the large variation of dispersion values at long wavelengths, which is illustrated in Fig. 3. The dispersion curves for the HALF structure except the hole-to-core separation  $S_{\text{hole}}$  are  $11.025 \mu\text{m}$  and  $12.225 \mu\text{m}$  and are marked by stars and circles, respectively. The dispersion curves for the HALF structure except the hole diameter  $\Phi_{\text{hole}}$  are  $0.7 \mu\text{m}$  and  $1.3 \mu\text{m}$  and are marked by triangles and squares, respectively. The larger hole diameter moves up the dispersion curve. It is observed that for  $\Phi_{\text{hole}} = 1.3 \mu\text{m}$ , the dispersion curve is also flat with near zero positive values.

Figure 4 illustrates the influence of the diameter and position of the assisting holes on the dispersion characteristics of the fiber. Specifically, the dispersion values and dispersion slope at  $\lambda = 1.55 \mu\text{m}$  are shown as functions of the air hole diameter  $\Phi_{\text{hole}}$  and the position  $S_{\text{hole}}$ . It is found in Fig. 4(a) that enlarging the air hole diameter  $\Phi_{\text{hole}}$  generally raises the dispersion values and dispersion slope. The proposed HALF structure with  $\Phi_{\text{hole}} = 1 \mu\text{m}$  has small negative dispersion value around  $-0.4 \text{ ps/nm-km}$  and negative dispersion slope around  $-0.01 \text{ ps/nm}^2\text{-km}$ . Further enlargement of the air holes would push the dispersion above zero and the dispersion slope to be positive. The position  $S_{\text{hole}}$  has a certain

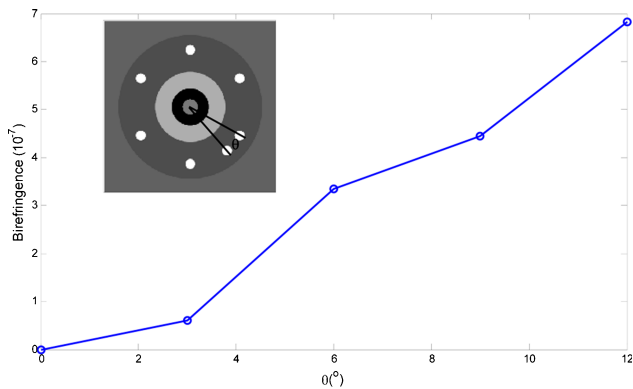


Fig. 5. (Color online) Birefringence value resulted from one displaced air hole with angular offset  $\theta$  to the original place. The schematic is shown in the inset.

contribution to modifying the dispersion characteristics as well. Specifically, moving away the air holes to the outer cladding results in smaller dispersion values and larger dispersion slope as shown in Fig. 4(b). The variation of dispersion values, and dispersion slope due to position parameter  $S_{\text{hole}}$ , is less significant than that of  $\Phi_{\text{hole}}$ . Appropriate selection of the air hole parameters can lead to an optimized design such as the NZ-DSF structure in this work.

The fabricated fiber may deviate from the design due to imperfection in fabrication technology. Therefore we also investigate the impact of air hole displacement on the birefringence. Specifically, we consider a single air hole that is displaced from its original place with angular offset  $\theta$ . The resulting birefringence is shown in Fig. 5. The pulse broadening due to the birefringence can be calculated by the equation  $\Delta\tau = BL/C$ , where  $\Delta\tau$  is the time delay characterizing the pulse broadening,  $B$  is the birefringence value,  $L$  is the fiber length, and  $C$  is the speed of light. When  $\theta$  is  $3^\circ$ , the birefringence of the fiber is about  $6 \times 10^{-8}$  at  $\lambda = 1.55 \mu\text{m}$ , resulting in pulse broadening of about 0.2 ps for every kilometer transmission in the fiber. It should be noted

that after long-haul transmission, the accumulated pulse broadening due to the birefringence has to be compensated.

#### 4. Conclusion

We have proposed a negative NZ-DSF design based on HALF's that exhibit low dispersion slope around  $-0.01 \text{ ps/nm}^2\text{-km}$  and small negative dispersion from 1530 to 1620 nm. This fiber design can have applications in broadband DWDM transmission systems.

This work was supported in part by the Agency for Science, Technology and Research (A\*STAR), Singapore.

#### References

1. J. C. Knight, T. A. Birks, P. St. J. Russell, and D. M. Atkin, "All-silica single-mode optical fiber with photonic crystal cladding," *Opt. Lett.* **21**, 1547–1549 (1996).
2. P. St. J. Russell, "Photonic crystal fibers," *J. Lightwave Technol.* **24**, 4729–4749 (2006).
3. T. Hasegawa, E. Sasaoka, M. Onishi, M. Nishimura, Y. Tsuji, and M. Koshiba, "Hole-assisted lightguide fiber for large anomalous dispersion and low optical loss," *Opt. Express* **9**, 681–686 (2001).
4. K. Saitoh, Y. Tsuchida, and M. Koshiba, "Bending-insensitive single-mode hole-assisted fibers with reduced splice loss," *Opt. Lett.* **30**, 1779–1781 (2005).
5. K. Saitoh, S. K. Varshney, and M. Koshiba, "Dispersion, birefringence, and amplification characteristics of newly designed dispersion compensating hole-assisted fibers," *Opt. Express* **15**, 17724–17735 (2007).
6. M. Yan, P. Shum, and C. Lu, "Hole-assisted multiring fiber with low dispersion around 1550 nm," *IEEE Photon. Technol. Lett.* **16**, 123–125 (2004).
7. F. Weling, D. L. A. Tjaden, and J. A. van Steenwijk, "The design of dispersion flattened single-mode fibers," in *Proceedings of the European Conference on Optical Communications (ECOC)* (Institution of Electrical Engineers, 1988), pp. 457–460.
8. X. Tian and X. Zhang, "Dispersion-flattened designs of the large effective-area single-mode fibers with ring index profiles," *Opt. Commun.* **230**, 105–113 (2004).